AIAA 2015-

On Possible Arc Inception on Low Voltage Solar Array

Boris Vayner*
Ohio Aerospace Institute, Cleveland, Ohio 44142

Abstract **Recent analysis of spacecraft failures during the period of 1990-2013 demonstrated clearly that electrostatic discharges caused more than 8% of all registered failures and anomalies, and comprised the most costly losses (25%) for operating companies and agencies. The electrostatic discharges on spacecraft surfaces are the results of differential charging above some critical (threshold) voltages. The mechanisms of differential charging are well known, and various methods have been developed to prevent a generation of significant electric fields in areas of triple junctions. For example, low bus voltages in Low Earth Orbit plasma environment and slightly conducting layer over coverglass (ITO) in Geosynchronous Orbit surroundings are believed to be quite reliable measures to prevent discharges on respective surfaces. In most cases, the vulnerable elements of spacecraft (solar arrays, diode boards, etc.) go through comprehensive ground tests in vacuum chambers. However, tests articles contain the miniscule fragments of spacecraft components such as 10-30 solar cells of many thousands deployed on spacecraft in orbit. This is one reason why manufacturing defects may not be revealed in ground tests but expose themselves in arcing on array surface in space. The other reason for ineffectiveness of discharge preventive measures is aging of all materials in harsh orbital environments. The expected life time of modern spacecraft varies within the range of five-fifteen years, and thermal cycling, radiation damages, and mechanical stresses can result in surface erosion on conductive layers and microscopic cracks in coverglass sheets and adhesive films. These possible damages may cause significant increases in local electric field strengths and subsequent discharges. The primary discharges may or may not be detrimental to spacecraft operation, but they can produce the necessary conditions for sustained arcs initiation. Multiple measures were developed to prevent sustained discharges between adjacent strings, and many ground tests were performed to determine threshold parameters (voltage and current) for sustained arcs. And again, manufacturing defects and aging in space environments may result in considerable decrease of critical threshold parameters. This paper is devoted to the analysis of possible reasons behind arcing on spacecraft with low bus voltages.**

Nomenclature

A	= area, m^2	n_e	= electron number density, m^{-3}
C_s	= capacitance, F/m^2	t	= time, s
E	= electric field, V/m	Φ	= potential, V
T_e	= electron temperature, eV	β	= enhancement factor,
U	= voltage, V	δ	= secondary electron emission yield
W	= electron energy, eV	ε	= dielectric permittivity
d	= coverglass thickness, m	σ	= conductivity, S/m
j_e	= electron current density, A/m^{-2}	τ	= relaxation time, s

*Senior Scientist, Boris.V.Vayner@nasa.gov, Member AIAA

1. INTRODUCTION

The magnitudes of differential charging depend on many factors: orbital environment, spacecraft design, operational voltage, material properties, temperature, and time in orbit. Subsequent discharges are responsible for significant part of failures and anomalies that cause substantial financial losses [1]. In order to prevent electrostatic discharges (or to mitigate their consequences) a spacecraft designer should possess reliable data regarding space environments and spacecraft material properties. Space plasma parameters are monitored with a quite satisfactory precision for Low Earth Orbit (LEO) and Geosynchronous Orbit (GEO) [2-4]. Relevant material properties have been under study for a long time but two main problems in this field are hold: entry of new materials, and changing material properties with time caused by long exposure to space environment [5]. There are two mutually supplemented approaches to determination of differential charging, arc thresholds, and expected arc rates on spacecraft in orbit: numerical simulations and ground tests in respective vacuum chambers. Significant contribution to the data base is made by space experiments (like MISSIE, for example) but high cost and obvious scope limitations restrict the volume of results concerning materials and space plasma parameters. Ground tests have obvious restrictions: only small parts of spacecraft can be tested in simulated environments, and simulated environments are different from orbital ones. That is why ground tests are supposed to provide "the worst conditions" in simulated environment where differential charging exceeds considerably the magnitudes expected in orbit. For example, in simulated GEO environment mono energetic electron beam (usually a few keV) is used to generate positive charging of dielectric surface. Such test setup excludes effect of radiation induced conductivity (RIC) that decreases differential potential in space [6]. In order to prevent detrimental results of differential charging in space all spacecraft elements that are prone to differential charging must be tested in the beginning of life and after artificial aging achieved by thermal cycling and irradiation in ground facilities. Essential features of such comprehensive tests are discussed below.

2. LEO SIMULATIONS

Differential charging in LEO plasma is caused by obvious requirement: net current collected by a spacecraft should be equal to zero in steady state conditions. The surfaces of dielectric parts exposed to the plasma acquire a low negative potential of a few volts due to low electron temperature. Floating potential of conductive surface of spacecraft body depends on solar array operational voltage, solar array design, and ratio of conductive and dielectric surface areas. The real magnitude of this potential may vary within rather wide range of 25-80% from operational voltage. Negative pole of a solar array is connected to s/c body (negative common ground), and significant potential difference can be originated between the interconnectors (cell edges) of the most negative cells and their coverglasses. The map of surface potential distribution for s/c in LEO can be obtained by computer modelling with appropriate software like NASCAP, SPISE, and MUSKAT but arcing threshold, collected current, and possibility of sustained arc initiation can be determined by ground tests in plasma chamber only. The test circuitry diagram, plasma parameters, and data acquiring system are described in Ref. 7. The results of tests for different solar array samples are shown in Tables 1&2 [8-10]. All these tests were performed under ambient temperature.

Table 1. List of solar array samples tested in two large chambers.

Sample No.(Type)	Coverglass Thickness (μm)	Coverglass Material	Overhang (μm)	Cell size (cm)	Interconnect
1(Si)	300	UVR	0	4x6	exposed
2(Si)	150	UVR	0	4x6	exposed
3(Si)	150	CMX UVR	0	4x6	exposed
4(Si)	150	UVR	250	4x6	exposed
5(Si)	150	UVR	0	8x8	wraptrough
6(TJ)	150	UVR	0	4x6	exposed
7(TJ)	150	UVR	0	4x6	exposed
8(TJ)	75	CMX	0	4x8	exposed
9(TJ)	75	CMX	0	4x8	exposed
10(TJ)	100	CMX	0	4x8	exposed

Table 2. Arc inception parameters.

Sample No.	Primary Arc Inception(V)	Sustained Arc Inception V	Sustained Arc Inception A
1	250	60	2.0
2	265	80	1.6
3	280		
4	340		
5	300(530)	>120	>4
6	170	80	2.25
7	200	50	2.0
		50	2.6
8	260		
9	>240		
10	220	100	>1.6

It is seen that arc thresholds for modern solar arrays exceed 200 V. Currently, the spacecraft operational voltages are well below this threshold, and one might conclude that electrostatic discharges on solar arrays do not present any hazard for their functioning. However, such a conclusion is wrong. First of all, when s/c is coming out of eclipse its solar array is cold (up to -100^{o} C) and voltage is about twice higher than operational one if the circuit is open. Arc threshold decreases significantly with decreasing temperature, and it may drop to 100-120 V negative (Fig.1). The second cause of arcing at low voltage is possible crack (or cavern) in adhesive layer developed due to multiple thermal cycles and mechanical stresses in orbit.

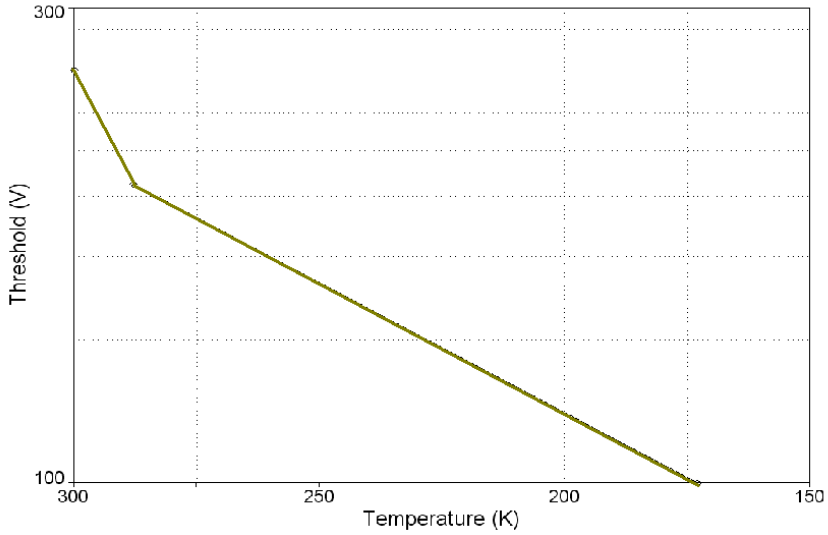

Fig.1. One example of decreasing arc threshold with temperature [11].

It is well known that the primary reason for electrostatic discharge is high electric field strength in the area of triple junction (interconnector-adhesive-plasma). This field strength can be calculated as following:
The potential difference between coverglass and underlying (semi)conductor is

$$U = E_1 d_1 + E_2 d_2 \qquad (1)$$

Where E_1 and E_2 are electric field strengths in adhesive and coverglass respectively; d_1 and d_2 are thicknesses of respective layers.

Border condition on adhesive/coverglass plane is

$$\varepsilon_1 E_1 = \varepsilon_2 E_2 \qquad (2)$$

Thus, electric field strength on the surface of (semi)conductor is

$$E_1 = \frac{\varepsilon_2}{\varepsilon_2 d_1 + \varepsilon_1 d_2} U \qquad (3)$$

Dielectric constant of adhesive material (DC93500) is equal to ε_1=3. Dielectric constant of coverglass depends on glass type but can be adopted as ε_2=5 for purposes of crude estimates. If there would be a small cavern in adhesive layer then the dielectric constant of vacuum (ε_c=1) should be substituted in Eq.3 for the calculation of electric field strength on (semi)conductor surface. For example, if d_1=50 μm and d_2=150 μm the field enhancement factor would be

$$\beta = \frac{E_{1c}}{E_1} = 1.75 \qquad (4)$$

For more contemporary arrays with thicknesses of respective layers of 25 μm and 125 μm the enhancement factor will reach β=2. The third factor influencing arc threshold magnitude is

outgassing of spacecraft structural elements. One test in controlled environment demonstrated the dependence of arc rate on water vapor partial pressure (Fig.2).

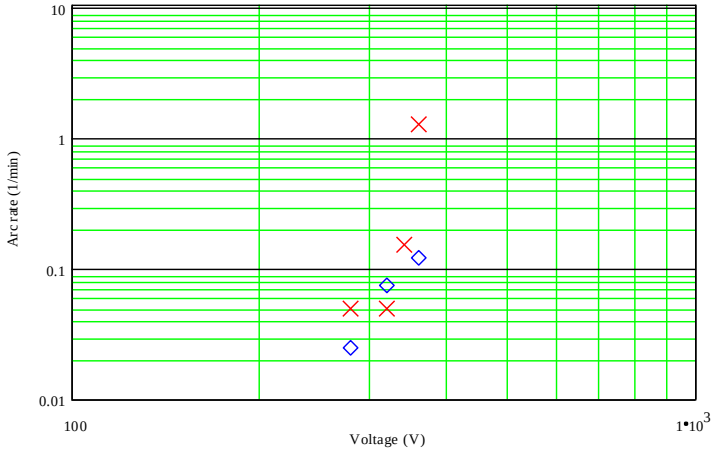

Fig.2. Arc rates were measured for two different water vapor partial pressures at 300 K: 0.26 µTorr (red) and 0.023 µTorr (blue) [12].

Thus, arcs on solar arrays with operational voltages above 100 V can be prevented by implementing special design features like wrapped through interconnectors or entire encapsulation of triple-junction areas.

3. GEO SIMULATIONS

Differential charging in GEO is caused by different reaction of dielectric and conductive materials to the irradiation with energetic electrons [2, p.16-19]. Spacecraft body (exposed conductive surface) in eclipse acquires the potential that is determined by the balance of electron and ion currents:

$$\Phi_{sc} = -\frac{T_e}{2}\ln\left(\frac{m_p}{m_e}\frac{T_e}{T_i}\right) \approx 3T_e \qquad (5)$$

The duration of charging process can be estimated as

$$\tau_{sc} = \frac{C_{sc}\cdot\Phi_{sc}}{j_e\cdot A} \qquad (6)$$

The real magnitude is varying within the wide range of 0.25-3 s depending on spacecraft dimensions and plasma parameters. The charging of coverglass is much slower and complicated process. First of all, the capacitance of solar array is about C_a=0.2-0.3 µF/m^2, and differential potential of U=1 kV can be reached during the time span of 30-300 s. In addition, secondary electron emission yield $\delta(W)$ for glass depends on primary electron energy and reaches peak factors of $\delta(W_m)$=5-8 for different materials [5,13]. Due to fast spacecraft body charging the electrons with energies only above s/c potential will reach the coverglass, and relations between

electron energy distribution and secondary yield characteristics come to interplay [4,14,15]. The appropriate differential charging on solar array sample in vacuum chamber can be reached by biasing strings with external power supply and irradiation the surface with monoenergetic electron beam. Steady state differential charging will be achieved when the energy of electrons is equal to the second crossover potential on *δ(W)* graph. Thus, the differential potential is

$$U = U_{bias} - \Phi_{cg} = U_{bias} - W_b + W_{sc} \qquad (7)$$

During all our tests the electron beam energy exceeded bias voltage on fixed value of 0.8 kV, and differential charging is expected to be independent on beam energy and beam current density:

$$U = W_{sc} - 0.8(kV) \qquad (8)$$

Second crossover energy is a tricky parameter that depends on temperature, incidence angle, and surface conditions. For our further discussion it seems quite satisfactory to adopt the magnitudes of 2.5-3 kV for glasses and 1-1.5 kV for RTV [16,17]. Differential potentials have been measured for different samples, and the results are shown in Fig.3.

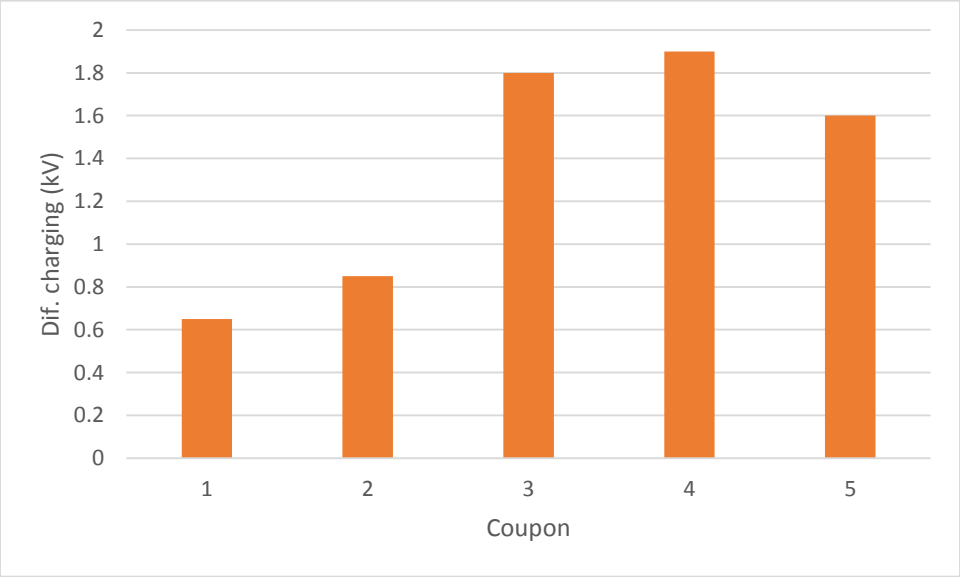

Fig.3 Differential charging is shown for samples from Table 1: 1-*##2&3 [18]; 2-##8&9 [9]; 3-#5 [19]; 4-#10 [10]; 5-new coupon [12]*.

Significant variations in differential potentials cannot be attributed to coverglass material properties (W_{sc}). For example, coupons #2&3 had the same coverglass as coupon #5 but difference in charging was about 1 kV. Moreover, the differential charging depended on bias voltage (beam energy) as it is shown in Fig.4. Increase of 1 kV in bias voltage caused increase in differential charging of about 0.2 kV. All coupons demonstrated arcing in GEO simulated conditions. According to the conventional theory of arc inception the discharge is initiated at the moment when electric field strength reaches a threshold magnitude [20,21]. An estimate for lower limit of charging time can be obtained by solving the equation for coverglass potential [22]. When the solar

Fig.4. Differential potentials are shown for coupon #5: left panel-U_b= -3 kV; right panel-U_b= -4 kV.

array surface is irradiated by an electron beam the coverglass potential increases according to the following equation:

$$C_s \frac{dU}{dt} = j_b(1-\delta(W_b - U_{cg})) \qquad (9)$$

Steady state is reached when the difference between the coverglass potential and electron beam energy is equal to the so called "second crossover" energy. In the neighborhood of this point the secondary electron emission yield can be represented in simple exponential form:

$$\delta(W) = \delta_m \exp\left(-\frac{W}{W_{sc}}\right) \qquad (10)$$

Substituting Eq.10 in Eq.9 and introducing dimensionless variables

$$\tau = \frac{j_b}{C_s W_{sc}} t \quad ; \quad \Phi = \frac{W_b - U_{cg}}{W_{sc}} \qquad (11)$$

one can obtain the solution shown in Fig.5.

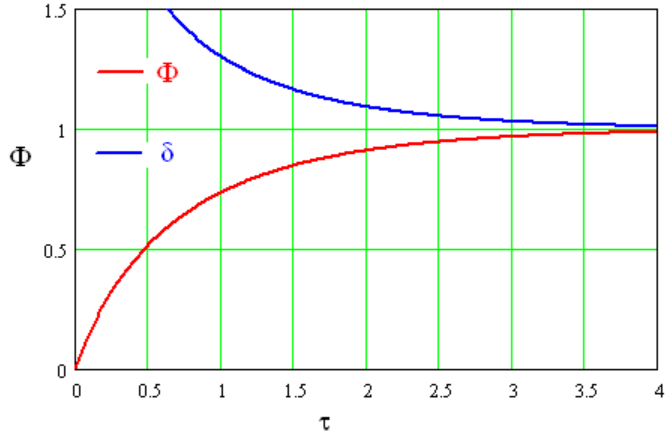

Fig.5. Sample is charging by an electron beam. Steady state voltage can be reached for a time span about τ=4.

For example, typical beam of 1 nA/cm^2 provides coverglass charging time a little more than 120 s. If second crossover energy is 2.0 kV [23], bias voltage is -2.5 kV, and beam energy is 3.3 kV then surface potential at steady state is U_{cg}= -1.3 kV, and differential charging reaches U= 1.2 kV. Measurements demonstrated a strongly nonlinear dependence of arc rate on electron beam current density (Fig.6).

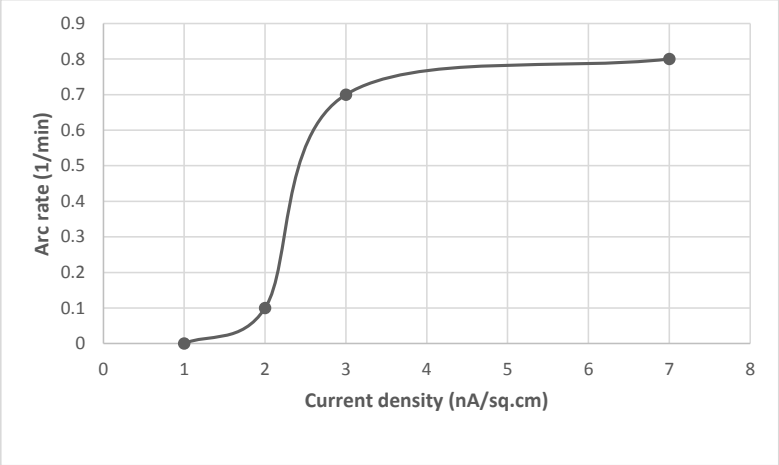

Fig.6. Arc rates were measured during 15 minutes irradiation time for each point.

The reasons for these discrepancy between measurements and theory are not clear now. One possible explanation could be attributed to the volume and surface conductivities of dielectrics involved-coverglass and adhesive. In reality, conductive current should be added to the right side of the Eq.(9):

$$j_c = \sigma \frac{U}{d_c} \qquad (12)$$

It is difficult to estimate the contribution of this current to the duration of charging process. For a typical glass conductivity of 10^{-13} S/m the conductive current density is below 0.06-0.1 nA/cm^2 under differential potential of 1 kV, and the contribution of conductive current to charging process (Eq.9) can be disregarded. However, coverglass surface contamination can influence the surface conductivity and the magnitude of second crossover energy. If ITO layer with conductivity of 10^{-9} S/m is used coverglass will never be charged to a high differential potential. Thus, the lower estimate for coverglass (with no ITO layer) charging time is a few minutes under GEO environment. The field enhancement caused by charging of side surfaces of dielectrics could be important for arc inception [24]. In simulated LEO conditions the current density of energetic electrons hitting side surface of dielectric is estimated as 1-2.5 nA/cm^2 [25]. This flux may provide the needed field enhancement, which explains a comparatively low arc threshold of 180-230 V. In simulated GEO environment the sharp increase of arc rate at beam current density above 2 nA/cm^2 may be caused by the same effect. It is worth noting that no RIC consequences were taken into account in experiments and theoretical estimates presented in this paper.

4. Conclusions

Electrostatic discharges on solar array surface can be initiated even on arrays with comparatively low operational voltages (around 100 V). RTV grouting the gaps between strings and interconnectors results in increasing thresholds but cannot guarantee absolute preventions of arcs [26, 27]. The most effective method for prevention of differential charging in GEO environment is ITO layer over coverglass but this method has such disadvantages as higher solar array cost and weight. Moreover, if spacecraft is supposed to fly through LEO and GEO then the deployment of ITO causes a sharp increase in current collection from ionosphere plasma and decrease in array efficiency [10,12]. The is no unique technique in preventing arcs: components of spacecraft power system must be undergone comprehensive tests in simulated environments corresponding to the spacecraft trajectory.

References

[1]. Landis, J. "Tabulation of Power-related Satellite Failure Causes", AIAA Paper 2013-3736, July 2013.

[2]. Garrett, H., and Whittlesey, A. "*Guide to Mitigating Spacecraft Charging Effects*", 2012, John Wiley & Sons, Inc., Hoboken, New Jersey, 178 pp.

[3]. NASA Technical Handbook, "*Mitigating In-Space Charging Effects-A Guideline*", NASA-STD-4002A, 2011.

[4]. Ferguson, D., Hilmer, R., and Davis, V. "Best Geosynchronous Earth Orbit Daytime Spacecraft Charging Index", *Journal of Spacecraft and Rockets*, Vol. 52, No. .., 2015, *pp.*

[5]. Dennison, JR. "Dynamic Interplay Between Spacecraft Charging, Space Environment Interactions and Evolving Materials", *IEEE Transactions on Plasma Science*, Vol. No., 2015, P.

[6]. Hanna, R., Paulmier, T., Molinie, P., Belhaj, M., Dirassen, B., Payan., and Balcon, N. "Radiation Induced Conductivity in Teflon FEP Irradiated With Multienergetic Electron Beam", *IEEE Transactions on Plasma Science*, Vol.41, No.12, 2013, P.3520-3525.

[7]. Vayner, B., Galofaro, J., and Ferguson, D. "Interactions of High-Voltage Solar Arrays with Their Plasma Environment: Ground Tests", *Journal of Spacecraft and Rockets*, Vol.41, No.6, 2004, P.1042-1050.

[8]. Vayner, B., Ferguson, D., and Galofaro J. "Detrimental Effects of Arcing on Solar Array Surfaces", 10th Spacecraft Charging Technology Conference, Biarritz, France, June 18-21, 2007.

[9]. Galofaro, J., Vayner, B., and Hillard, G. "Experimental Tests of UltraFlex Array Designs in Low Earth Orbital and Geosynchronous Charging Environments", AIAA Paper 2009-3525, June 2009.

[10].Vayner, B. "TEST of NEW COUPON", Final Report, June 2013 (unpublished).

[11]. Vayner, B., and Galofaro, J. "ARCING ON SOLAR ARRAYS AT LOW TEMPERATURES", AIAA Paper 2010-75, Orlando, Florida, Jan. 2010.

[12].Vayner, B. "Tests of 2-String Coupons in LEO/GEO Simulated Environments", Final Report, April 2014 (unpublished).

[13].Scholtz, J., Dijkkamp, D., and Schmitz, R. "Secondary Electron Emission Properties", *Philips Journal of Research*, Vol.50, 1996, pp. 375-389.

[14].Lai,S., and Della-Rose, D. "Spacecraft Charging at Geosynchronous Altitudes: New

Evidence for Existence of Critical Temperature", *Journal of Spacecraft and Rockets*, Vol. 38, No.4, 2001, pp.922-928.
[15]. Likar, J., Bogorad, A., August, K. et al. "Spacecraft Chjarging, Plume Interactions, and Space Radiation Design Considerations for All-Electric GEO Satellite Missions", *IEEE Transactions on Plasma Science*, Vol. 43, 2015, in press.
[16].Balcon, N., Payan, D., Belhaj, M., Tondu, T., and Inguimbert, V. "Secondary Electron Emission on Space Materials", *IEEE Transactions on Plasma Science*, Vol.40, No.2, 2012, pp.282-290.
[17].Thomson, C., Zavyalov, V.,Dennison, J., and Corbridge, J. "Electron Emission Properties of Insulator Materials Pertinent to the International Space Station", 9th Spacecraft Charging Technology Conference, Tsukuba, Japan, April 4-8, 2005, 24 pp.
[18]. Vayner, B., Galofaro, J., and Ferguson, D. "COMPARATIVE ANALYSIS of ARCING in LEO and GEO SIMULATED ENVIRONMENTS", AIAA Paper 2007-0093, Jan.2007.
[19]. Vayner, B., Ferguson, C. et al. "Further Results From the US Round-Robin Experiment on Plasma Expansion Speed", AIAA Paper 2013-0809, Jan. 2013.
[20]. Hastings,D.E., Weyl,G., and Kaufman, D. "Threshold Voltage for Arcing on Negatively Biased Solar Arrays", *Journal of Spacecraft and Rockets*, Vol.27, No.5, 1990, pp.539-544.
[21].Cho,M., and Hastings, D.E. "Computer Particle Simulation on High-Voltage Solar Array Arcing Onset", *Journal of Spacecraft and Rockets*, Vol.30, No.2, 1993, pp.189-205.
[22]. Vayner, B., Ferguson, D., and Galofaro, J. "THE EFFECT OF SOLAR ARRAY SIZE ON SUSTAINED ARC INCEPTION", AIAA Paper 2009-0115, Jan.2009.
[23]. Mueller, C.W. "The Secondary Electron Emission of Pyrex Glass", *Journal of Applied Physics*, Vol.16, No.8, 1945, pp.453-458.
[24]. Nevrovsky, V.A. "Analysis of Elementary Processes Leading to Surface Flashover in Vacuum", Proceedings of XVIIIth International Symp. on Discharges and Electrical Insulation in Vacuum, Eindhoven, The Netherlands, Vol.1, Aug.17-21, 1998, pp.159-161.
[25]. Vayner, B., Galofaro, J., and Ferguson, D. "Interactions of High-Voltage Solar Arrays with Their Plasma Environment: Physical Processes", *Journal of Spacecraft and Rockets*, Vol.41, No.6, 2004, pp.1031-1041.
[26]. Vayner, B., and Galofaro, J. "Inception and Prevention of Sustained Discharges on Solar Arrays", 11th Spacecraft Charging Technology Conference, June 20-24, 2010, Albuquerque, NM.
[27]. Wright, K., Schneider, T., Vaughn, J., Hoang, B., Funderburk, V., Wong, F., and Gardiner, G. " Electrostatic Discharge Testing of Multi-Junction Solar Array Coupons after Combined Space Environmental Exposures", *IEEE Transactions on Plasma Science*, Vol. 40, No.2, 2012, pp.334-344.